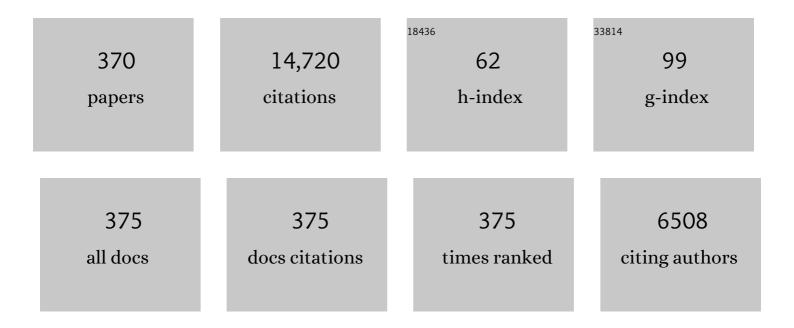
Christian Mitterer

List of Publications by Year in descending order

Source: https://exaly.com/author-pdf/6113197/publications.pdf Version: 2024-02-01



#	Article	IF	CITATIONS
1	Microstructural design of hard coatings. Progress in Materials Science, 2006, 51, 1032-1114.	16.0	793
2	Self-organized nanostructures in the Ti–Al–N system. Applied Physics Letters, 2003, 83, 2049-2051.	1.5	529
3	Thermal stability of Al–Cr–N hard coatings. Scripta Materialia, 2006, 54, 1847-1851.	2.6	224
4	Microstructure and mechanical/thermal properties of Cr–N coatings deposited by reactive unbalanced magnetron sputtering. Surface and Coatings Technology, 2001, 142-144, 78-84.	2.2	207
5	Self-organized nanocolumnar structure in superhard TiB2 thin films. Applied Physics Letters, 2005, 86, 131909.	1.5	192
6	A comparative study on reactive and non-reactive unbalanced magnetron sputter deposition of TiN coatings. Thin Solid Films, 2002, 415, 151-159.	0.8	190
7	Vanadium containing self-adaptive low-friction hard coatings for high-temperature applications: A review. Surface and Coatings Technology, 2013, 228, 1-13.	2.2	190
8	Oxidation of vanadium nitride and titanium nitride coatings. Surface Science, 2007, 601, 1153-1159.	0.8	186
9	Structure, mechanical and tribological properties of sputtered Ti1–xAlxN coatings with 0.5â‰ ¤ â‰ 9 .75. Surface and Coatings Technology, 2005, 200, 2358-2365.	2.2	181
10	Borides in Thin Film Technology. Journal of Solid State Chemistry, 1997, 133, 279-291.	1.4	180
11	Application of hard coatings in aluminium die casting — soldering, erosion and thermal fatigue behaviour. Surface and Coatings Technology, 2000, 125, 233-239.	2.2	175
12	Microstructure and properties of nanocomposite Ti–B–N and Ti–B–C coatings. Surface and Coatings Technology, 1999, 120-121, 405-411.	2.2	170
13	Sputter deposition of ultrahard coatings within the system Ti-B-C-N. Surface and Coatings Technology, 1990, 41, 351-363.	2.2	161
14	Magnéli phase formation of PVD Mo–N and W–N coatings. Surface and Coatings Technology, 2006, 201, 3335-3341.	2.2	159
15	The origin of stresses in magnetron-sputtered thin films with zone T structures. Acta Materialia, 2010, 58, 2621-2633.	3.8	152
16	Influence of high-temperature oxide formation on the tribological behaviour of TiN and VN coatings. Wear, 2007, 262, 1152-1158.	1.5	151
17	Structure–property relationships in single- and dual-phase nanocrystalline hard coatings. Surface and Coatings Technology, 2003, 174-175, 725-731.	2.2	148
18	Calorimetric evidence for frictional self-adaptation of TiAlN/VN superlattice coatings. Surface and Coatings Technology, 2004, 177-178, 341-347.	2.2	142

#	Article	IF	CITATIONS
19	Structure and properties of hard and superhard Zr–Cu–N nanocomposite coatings. Materials Science & Engineering A: Structural Materials: Properties, Microstructure and Processing, 2000, 289, 189-197.	2.6	139
20	Oxidation kinetics of sputtered Cr–N hard coatings. Surface and Coatings Technology, 2001, 146-147, 222-228.	2.2	125
21	A new low-friction concept for Ti1â^'xAlxN based coatings in high-temperature applications. Surface and Coatings Technology, 2004, 188-189, 358-363.	2.2	120
22	Thermal stability of sputtered Al2O3 coatings. Surface and Coatings Technology, 2010, 204, 1576-1581.	2.2	119
23	High-temperature properties of nanocomposite TiBxNy and TiBxCy coatings. Surface and Coatings Technology, 2000, 133-134, 131-137.	2.2	117
24	Advanced characterization methods for wear resistant hard coatings: A review on recent progress. Surface and Coatings Technology, 2016, 285, 31-46.	2.2	116
25	A New Low Friction Concept for High Temperatures: Lubricious Oxide Formation on Sputtered VN Coatings. Tribology Letters, 2004, 17, 751-756.	1.2	115
26	Thermal stability of PVD hard coatings. Vacuum, 2003, 71, 279-284.	1.6	113
27	Experiment and simulation of the compositional evolution of Ti–B thin films deposited by sputtering of a compound target. Journal of Applied Physics, 2008, 104, .	1.1	112
28	Low-friction TiN–MoS2 coatings produced by dc magnetron co-deposition. Surface and Coatings Technology, 1998, 108-109, 345-351.	2.2	111
29	Energetic balance and kinetics for the decomposition of supersaturated Tilâ^'xAlxN. Acta Materialia, 2007, 55, 1441-1446.	3.8	106
30	Influence of oxide phase formation on the tribological behaviour of Ti–Al–V–N coatings. Surface and Coatings Technology, 2005, 200, 1731-1737.	2.2	103
31	X-ray nanodiffraction reveals strain and microstructure evolution in nanocrystalline thin films. Scripta Materialia, 2012, 67, 748-751.	2.6	103
32	Nanoporous activated carbon cloth as a versatile material for hydrogen adsorption, selective gas separation and electrochemical energy storage. Nano Energy, 2017, 40, 49-64.	8.2	101
33	Low-stress superhard Tiî—,B films prepared by magnetron sputtering. Surface and Coatings Technology, 2003, 174-175, 744-753.	2.2	97
34	Abrasive wear of high speed steels: Influence of abrasive particles and primary carbides on wear resistance. Tribology International, 2003, 36, 765-770.	3.0	95
35	Industrial applications of PACVD hard coatings. Surface and Coatings Technology, 2003, 163-164, 716-722.	2.2	89
36	Improved oxidation resistance of TiAlN coatings by doping with Si or B. Surface and Coatings Technology, 2009, 203, 3104-3110.	2.2	86

#	Article	IF	CITATIONS
37	Non-reactively sputtered TiN and TiB2 films: influence of activation energy on film growth. Surface and Coatings Technology, 1997, 97, 567-573.	2.2	84
38	High-Temperature Tribological Behavior of CrN-Ag Self-lubricating Coatings. Advanced Engineering Materials, 2006, 8, 1125-1129.	1.6	81
39	Finite element simulation of the effect of surface roughness on nanoindentation of thin films with spherical indenters. Surface and Coatings Technology, 2007, 202, 1103-1107.	2.2	79
40	Structure–property relations of arc-evaporated Al–Cr–Si–N coatings. Surface and Coatings Technology, 2008, 202, 3555-3562.	2.2	78
41	Size effect of thermal expansion and thermal/intrinsic stresses in nanostructured thin films: Experiment and model. Acta Materialia, 2011, 59, 6631-6645.	3.8	77
42	Multifunctional multi-component PVD coatings for cutting tools. Surface and Coatings Technology, 2005, 200, 1867-1871.	2.2	75
43	On the effect of Ta on improved oxidation resistance of Ti–Al–Ta–N coatings. Journal of Vacuum Science and Technology A: Vacuum, Surfaces and Films, 2009, 27, 554-560.	0.9	74
44	Cathodic arc deposition of (Al,Cr)2O3: Macroparticles and cathode surface modifications. Surface and Coatings Technology, 2011, 206, 1454-1460.	2.2	74
45	The Beneficial Effect of High-Temperature Oxidation on the Tribological Behaviour of V and VN Coatings. Tribology Letters, 2007, 28, 1-7.	1.2	72
46	Age hardening of PACVD TiBN thin films. Scripta Materialia, 2005, 53, 241-245.	2.6	71
47	Annealing of intrinsic stresses in sputtered TiN films: The role of thickness-dependent gradients of point defect density. Surface and Coatings Technology, 2007, 201, 4777-4780.	2.2	71
48	Grain boundary design of thin films: Using tilted brittle interfaces for multiple crack deflection toughening. Acta Materialia, 2017, 122, 130-137.	3.8	71
49	Microstructure and properties of nitride and diboride hard coatings deposited under intense mild-energy ion bombardment. Surface and Coatings Technology, 1999, 116-119, 133-140.	2.2	70
50	The effect of oxide-forming alloying elements on the high temperature wear of a hot work steel. Wear, 2005, 258, 1491-1499.	1.5	70
51	TiAlN based nanoscale multilayer coatings designed to adapt their tribological properties at elevated temperatures. Thin Solid Films, 2005, 485, 160-168.	0.8	70
52	High-temperature low-friction properties of vanadium-alloyed AlCrN coatings. Tribology Letters, 2006, 23, 101-107.	1.2	70
53	Mechanical Size-Effects in Miniaturized and Bulk Materials. Advanced Engineering Materials, 2006, 8, 1033-1045.	1.6	70
54	Structure and properties of TiB2 based coatings prepared by unbalanced DC magnetron sputtering. Surface and Coatings Technology, 1998, 98, 1483-1489.	2.2	69

#	Article	IF	CITATIONS
55	The influence of bias voltage on structure and mechanical/tribological properties of arc evaporated Ti–Al–V–N coatings. Surface and Coatings Technology, 2007, 202, 1050-1054.	2.2	68
56	The effect of deposition temperature on microstructure and properties of thermal CVD TiN coatings. International Journal of Refractory Metals and Hard Materials, 2008, 26, 120-126.	1.7	67
57	The effect of droplets in arc evaporated TiAlTaN hard coatings on the wear behavior. Surface and Coatings Technology, 2014, 257, 95-101.	2.2	67
58	Nanocrystalline hard coatings within the quasi-binary system TiN–TiB2. Vacuum, 1998, 50, 313-318.	1.6	66
59	Structure–property relations in ZrCN coatings for tribological applications. Surface and Coatings Technology, 2010, 205, 2134-2141.	2.2	65
60	Electrodeposited Nanostructured CoFe2O4 for Overall Water Splitting and Supercapacitor Applications. Catalysts, 2019, 9, 176.	1.6	65
61	Hard coatings produced by PACVD applied to aluminium die casting. Surface and Coatings Technology, 1999, 116-119, 530-536.	2.2	64
62	Tribological Properties of TiN/Ag Nanocomposite Coatings. Tribology Letters, 2008, 30, 53-60.	1.2	63
63	Low-friction TiN coatings deposited by PACVD. Surface and Coatings Technology, 2003, 163-164, 451-456.	2.2	62
64	Microstructural aspects determining the adhesive wear of tool steels. Wear, 2006, 260, 1028-1034.	1.5	61
65	Nanocomposite Ti–B–N coatings synthesized by reactive arc evaporation. Acta Materialia, 2006, 54, 4193-4200.	3.8	61
66	A novel approach for determining fracture toughness of hard coatings on the micrometer scale. Scripta Materialia, 2012, 67, 708-711.	2.6	61
67	Oxidation of arc-evaporated Al1â [~] 'xCrxN coatings. Journal of Vacuum Science and Technology A: Vacuum, Surfaces and Films, 2007, 25, 711-720.	0.9	60
68	Fracture toughness enhancement of brittle nanostructured materials by spatial heterogeneity: A micromechanical proof for CrN/Cr and TiN/SiOx multilayers. Materials and Design, 2016, 104, 227-234.	3.3	60
69	Structure–property relations in Cr–C/a-C:H coatings deposited by reactive magnetron sputtering. Surface and Coatings Technology, 2005, 200, 1147-1150.	2.2	59
70	Arc Evaporation of Ti–Al–Ta–N Coatings: The Effect of Bias Voltage and Ta on High-temperature Tribological Properties. Tribology Letters, 2008, 30, 91-97.	1.2	59
71	Origins of microstructure and stress gradients in nanocrystalline thin films: The role of growth parameters and self-organization. Acta Materialia, 2013, 61, 6255-6266.	3.8	59
72	Self-Organized Nanostructures in Hard Ceramic Coatings. Advanced Engineering Materials, 2005, 7, 1071-1082.	1.6	58

#	Article	IF	CITATIONS
73	Thermal decomposition routes of CrN hard coatings synthesized by reactive arc evaporation and magnetron sputtering. Thin Solid Films, 2008, 517, 568-574.	0.8	58
74	Sputter deposition of wear-resistant coatings within the system Zrî—,Bî—,N. Materials Science & Engineering A: Structural Materials: Properties, Microstructure and Processing, 1991, 140, 670-675.	2.6	57
75	3D versus 2D finite element simulation of the effect of surface roughness on nanoindentation of hard coatings. Surface and Coatings Technology, 2009, 203, 3286-3290.	2.2	57
76	Finite element study of the influence of hard coatings on hard metal tool loading during milling. Surface and Coatings Technology, 2016, 304, 134-141.	2.2	57
77	Structural and mechanical properties of dc and pulsed dc reactive magnetron sputtered V ₂ O ₅ films. Journal Physics D: Applied Physics, 2007, 40, 7716-7719.	1.3	55
78	The effect of increasing V content on structure, mechanical and tribological properties of arc evaporated Ti–Al–V–N coatings. International Journal of Refractory Metals and Hard Materials, 2009, 27, 502-506.	1.7	55
79	Structure-hardness relations in sputtered Ti–Al–V–N films. Thin Solid Films, 2003, 444, 189-198.	0.8	54
80	X-ray nanodiffraction reveals stress distribution across an indented multilayered CrN–Cr thin film. Acta Materialia, 2015, 85, 24-31.	3.8	53
81	A transmission electron microscopy study on sputtered Zrî—,B and Zrî—,Bî—,N films. Thin Solid Films, 1991, 201, 123-135.	0.8	52
82	Annealing studies of nanocomposite Ti–Si–C thin films with respect to phase stability and tribological performance. Materials Science & Engineering A: Structural Materials: Properties, Microstructure and Processing, 2006, 429, 90-95.	2.6	52
83	In-situ Observation of Cross-Sectional Microstructural Changes and Stress Distributions in Fracturing TiN Thin Film during Nanoindentation. Scientific Reports, 2016, 6, 22670.	1.6	52
84	Microstructure and mechanical properties of CVD TiN/TiBN multilayer coatings. Surface and Coatings Technology, 2019, 370, 311-319.	2.2	52
85	Co-sputtered films within the quasi-binary system TiN-TiB2. Surface and Coatings Technology, 1997, 94-95, 297-302.	2.2	51
86	30 nm X-ray focusing correlates oscillatory stress, texture and structural defect gradients across multilayered TiN-SiOx thin film. Acta Materialia, 2018, 144, 862-873.	3.8	51
87	Hard coatings for cutting applications: Physical vs. chemical vapor deposition and future challenges for the coatings community. Surface and Coatings Technology, 2022, 429, 127949.	2.2	51
88	Thermally induced self-hardening of nanocrystalline Ti–B–N thin films. Journal of Applied Physics, 2006, 100, 044301.	1.1	50
89	Structure and stability of phases within the NbN–AlN system. Journal Physics D: Applied Physics, 2010, 43, 145403.	1.3	49
90	Structure of sputtered nanocomposite CrC[sub x]â^•a-C:H thin films. Journal of Vacuum Science & Technology B, 2006, 24, 1837.	1.3	48

#	Article	IF	CITATIONS
91	Influence of Al and Si content on structure and mechanical properties of arc evaporated Al–Cr–Si–N thin films. Thin Solid Films, 2013, 534, 403-409.	0.8	48
92	Radioâ€frequency sputter deposition of boron nitride based thin films. Journal of Vacuum Science and Technology A: Vacuum, Surfaces and Films, 1989, 7, 2646-2651.	0.9	46
93	Microstructure, mechanical and tribological properties of PACVD Ti(B,N) and TiB2 coatings. Surface and Coatings Technology, 2003, 174-175, 1229-1233.	2.2	46
94	Self-organized periodic soft-hard nanolamellae in polycrystalline TiAlN thin films. Thin Solid Films, 2013, 545, 29-32.	0.8	46
95	Corrosion of zirconium boride and zirconium boron nitride coated steels. Surface and Coatings Technology, 1995, 71, 60-66.	2.2	45
96	Oxidation behaviour and tribological properties of arc-evaporated ZrAlN hard coatings. Surface and Coatings Technology, 2012, 206, 2337-2345.	2.2	45
97	Tribological properties of Al2O3 hard coatings modified by mechanical blasting and polishing post-treatment. Wear, 2012, 289, 9-16.	1.5	45
98	Sputter deposition of decorative boride coatings. Vacuum, 1995, 46, 1281-1294.	1.6	44
99	The influence of the ion bombardment on the optical properties of TiNx and ZrNx coatings. Surface and Coatings Technology, 1998, 108-109, 230-235.	2.2	44
100	Thermal stability of nanocomposite CrC/a-C:H thin films. Thin Solid Films, 2007, 515, 5411-5417.	0.8	44
101	Origin of temperature-induced low friction of sputtered Si-containing amorphous carbon coatings. Acta Materialia, 2015, 82, 437-446.	3.8	43
102	The electro-mechanical behavior of sputter-deposited Mo thin films on flexible substrates. Thin Solid Films, 2016, 606, 45-50.	0.8	43
103	Al-rich cubic Al0.8Ti0.2N coating with self-organized nano-lamellar microstructure: Thermal and mechanical properties. Surface and Coatings Technology, 2016, 291, 89-93.	2.2	42
104	Characterization of tribo-layers on self-lubricating plasma-assisted chemical-vapor-deposited TiN coatings. Thin Solid Films, 2004, 460, 125-132.	0.8	40
105	Thermal stability of magnetron sputtered Zr–Si–N films. Surface and Coatings Technology, 2006, 201, 3368-3376.	2.2	40
106	Hardness evolution of Al–Cr–N coatings under thermal load. Journal of Materials Research, 2008, 23, 2880-2885.	1.2	40
107	Texture development in polycrystalline CrN coatings: the role of growth conditions and a Cr interlayer. Journal Physics D: Applied Physics, 2009, 42, 075401.	1.3	40
108	Sputtered molybdenum films: Structure and property evolution with film thickness. Vacuum, 2014, 99, 149-152.	1.6	39

#	Article	IF	CITATIONS
109	Fatigue properties of Ti-based hard coatings deposited onto tool steels. Surface and Coatings Technology, 2001, 142-144, 117-124.	2.2	38
110	Recrystallization and grain growth of nanocomposite Ti–B–N coatings. Thin Solid Films, 2003, 440, 174-179.	0.8	38
111	Structure–property–performance relations of high-rate reactive arc-evaporated Ti–B–N nanocomposite coatings. Surface and Coatings Technology, 2006, 201, 2553-2559.	2.2	38
112	High-temperature tribological behaviour of sputtered NbNx thin films. Surface and Coatings Technology, 2007, 202, 1017-1022.	2.2	38
113	Effect of nitrogen-incorporation on structure, properties and performance of magnetron sputtered CrB2. Surface and Coatings Technology, 2008, 202, 3088-3093.	2.2	38
114	Influence of phase transition on the tribological performance of arc-evaporated AlCrVN hard coatings. Surface and Coatings Technology, 2009, 203, 1101-1105.	2.2	38
115	Nanoporous polymer-derived activated carbon for hydrogen adsorption and electrochemical energy storage. Chemical Engineering Journal, 2022, 427, 131730.	6.6	38
116	CO addition in low-pressure chemical vapour deposition of medium-temperature TiCxN1-x based hard coatings. Surface and Coatings Technology, 2011, 206, 1691-1697.	2.2	37
117	Lateral gradients of phases, residual stress and hardness in a laser heated Ti0.52Al0.48N coating on hard metal. Surface and Coatings Technology, 2012, 206, 4502-4510.	2.2	37
118	Residual stress gradients in α-Al2O3 hard coatings determined by pencil-beam X-ray nanodiffraction: The influence of blasting media. Surface and Coatings Technology, 2015, 262, 134-140.	2.2	37
119	Few-layer graphene-like flakes derived by plasma treatment: A potential material for hydrogen adsorption and storage. Microporous and Mesoporous Materials, 2016, 225, 482-487.	2.2	37
120	Investigation of the origin of compressive residual stress in CVD TiB 2 hard coatings using synchrotron X-ray nanodiffraction. Surface and Coatings Technology, 2014, 258, 121-126.	2.2	36
121	Cu diffusion in single-crystal and polycrystalline TiN barrier layers: A high-resolution experimental study supported by first-principles calculations. Journal of Applied Physics, 2015, 118, .	1.1	36
122	Thickness dependence of the electro-mechanical response of sputter-deposited Mo thin films on polyimide: Insights from in situ synchrotron diffraction tensile tests. Materials Science & Engineering A: Structural Materials: Properties, Microstructure and Processing, 2017, 697, 17-23.	2.6	36
123	PACVD TiN/Ti–B–N multilayers: from micro- to nano-scale. Surface and Coatings Technology, 2004, 177-178, 348-354.	2.2	35
124	High-temperature tribology and oxidation of Ti1â^'xâ^'yAlxTayN hard coatings. Surface and Coatings Technology, 2018, 342, 190-197.	2.2	35
125	Evolution of structure and residual stress of a fcc/hex-AlCrN multi-layered system upon thermal loading revealed by cross-sectional X-ray nano-diffraction. Acta Materialia, 2019, 162, 55-66.	3.8	35
126	Experimental studies on epitaxially grown TiN and VN films. Thin Solid Films, 2007, 516, 369-373.	0.8	34

#	Article	IF	CITATIONS
127	Tribological Properties of Reactive Magnetron Sputtered V2O5 and VN–V2O5 Coatings. Tribology Letters, 2008, 30, 21-26.	1.2	34
128	Cross-sectional structure-property relationship in a graded nanocrystalline Ti1â^'xAlxN thin film. Acta Materialia, 2016, 102, 212-219.	3.8	34
129	Effects of reference materials on texture coefficients determined for a CVD α-Al2O3 coating. Surface and Coatings Technology, 2019, 359, 314-322.	2.2	34
130	Microstructural evolution and thermal stability of AlCr(Si)N hard coatings revealed by in-situ high-temperature high-energy grazing incidence transmission X-ray diffraction. Acta Materialia, 2020, 186, 545-554.	3.8	34
131	Hard and superhard nanocomposite Al–Cu–N films prepared by magnetron sputtering. Surface and Coatings Technology, 2001, 142-144, 603-609.	2.2	33
132	Comparative study of Ti1â^'xAlxN coatings alloyed with Hf, Nb, and B. Surface and Coatings Technology, 2005, 200, 113-117.	2.2	33
133	The nanostructure, wear and corrosion performance of arc-evaporated CrBxNy nanocomposite coatings. Surface and Coatings Technology, 2009, 204, 246-255.	2.2	33
134	Microstructure and thermal stability of corundum-type (Al0.5Cr0.5)2O3 solid solution coatings grown by cathodic arc evaporation. Thin Solid Films, 2013, 534, 373-379.	0.8	33
135	Seed layer stimulated growth of crystalline high Al containing (Al,Cr)2O3 coatings deposited by cathodic arc evaporation. Thin Solid Films, 2014, 550, 95-104.	0.8	33
136	Phase composition and thermal stability of arc evaporated Ti1â^'xAlxN hard coatings with 0.4 ≤ ≤0.67. Surface and Coatings Technology, 2017, 309, 687-693.	2.2	33
137	Tribological behavior of PACVD TiN coatings in the temperature range up to 500 °C. Surface and Coatings Technology, 2003, 163-164, 585-590.	2.2	32
138	Structural investigations of aluminum-chromium-nitride hard coatings by Raman micro-spectroscopy. Thin Solid Films, 2006, 515, 2197-2202.	0.8	32
139	Formation mechanisms of low-friction tribo-layers on arc-evaporated TiC1â^'xNx hard coatings. Wear, 2008, 265, 525-532.	1.5	32
140	Thermal crack network on CVD TiCN/α-Al2O3 coated cemented carbide cutting tools. International Journal of Refractory Metals and Hard Materials, 2019, 81, 1-6.	1.7	32
141	Thermal crack formation in TiCN/α-Al2O3 bilayer coatings grown by thermal CVD on WC-Co substrates with varied Co content. Surface and Coatings Technology, 2020, 392, 125687.	2.2	32
142	Synthesis–structure–property relations for Cr–B–N coatings sputter deposited reactively from a Cr–B target with 20at% B. Vacuum, 2008, 82, 771-776.	1.6	31
143	Structural and mechanical properties of diamond-like carbon films deposited by an anode layer source. Thin Solid Films, 2009, 517, 6502-6507.	0.8	31
144	Abrasive and Adhesive Wear Behavior of Arc-Evaporated Al1â^'x CrxN Hard Coatings. Tribology Letters, 2010, 37, 605-611.	1.2	31

#	Article	IF	CITATIONS
145	Microstructure–property relations of reactively magnetron sputtered VCxNy films. Surface and Coatings Technology, 2011, 205, 3805-3809.	2.2	31
146	Sputtered Si-containing low-friction carbon coatings for elevated temperatures. Tribology International, 2014, 77, 15-23.	3.0	31
147	Nanoindentation of chemical-vapor deposited Al2O3 hard coatings at elevated temperatures. Thin Solid Films, 2015, 578, 20-24.	0.8	31
148	Plasma-assisted pre-treatment for PACVD TiN coatings on tool steel. Surface and Coatings Technology, 2003, 174-175, 687-693.	2.2	30
149	Nanocomposite coatings within the system Ti–B–N deposited by plasma assisted chemical vapor deposition. Journal of Vacuum Science & Technology an Official Journal of the American Vacuum Society B, Microelectronics Processing and Phenomena, 2003, 21, 1084.	1.6	30
150	Stress evolution in CrN/Cr coating systems during thermal straining. Thin Solid Films, 2008, 516, 1972-1976.	0.8	30
151	Influence of residual stresses and grain size on the spinodal decomposition of metastable Ti1â^'xAlxN coatings. Surface and Coatings Technology, 2012, 209, 190-196.	2.2	30
152	Synthesis of nanoporous graphene oxide adsorbents by freeze-drying or microwave radiation: Characterization and hydrogen storage properties. International Journal of Hydrogen Energy, 2015, 40, 6844-6852.	3.8	30
153	The effect of B and C addition on microstructure and mechanical properties of TiN hard coatings grown by chemical vapor deposition. Thin Solid Films, 2019, 688, 137283.	0.8	30
154	Interlayer thickness influence on the tribological response of bi-layer coatings. Tribology International, 2010, 43, 108-112.	3.0	29
155	Cross-sectional X-ray nanobeam diffraction analysis of a compositionally graded CrNx thin film. Thin Solid Films, 2013, 542, 1-4.	0.8	29
156	Influence of pulsed bias duty cycle variations on structural and mechanical properties of arc evaporated (Al,Cr)2O3 coatings. Surface and Coatings Technology, 2015, 282, 43-51.	2.2	29
157	Structure evolution in reactively sputtered molybdenum oxide thin films. Vacuum, 2016, 131, 246-251.	1.6	29
158	Substrate and coating damage by arcing during sputtering. Surface and Coatings Technology, 1997, 89, 233-238.	2.2	28
159	The influence of boron content on the tribological performance of Ti–N–B coatings prepared by thermal CVD. Surface and Coatings Technology, 2006, 201, 4247-4252.	2.2	28
160	Solvothermal synthesis, nanostructural characterization and gas cryo-adsorption studies in a metal–organic framework (IRMOF-1) material. International Journal of Hydrogen Energy, 2017, 42, 23899-23907.	3.8	28
161	Influence of cutting speed and workpiece material on the wear mechanisms of CVD TiCN/α-Al2O3 coated cutting inserts during turning. Wear, 2018, 398-399, 90-98.	1.5	28
162	Investigations on the effects of plasma-assisted pre-treatment for plasma-assisted chemical vapour deposition TiN coatings on tool steel. Thin Solid Films, 2004, 461, 277-281.	0.8	27

#	Article	IF	CITATIONS
163	Titanium doped CVD alumina coatings. Surface and Coatings Technology, 2008, 203, 350-356.	2.2	27
164	Structure, mechanical properties and oxidation behaviour of arc-evaporated NbAlN hard coatings. Surface and Coatings Technology, 2010, 204, 2447-2453.	2.2	27
165	Residual stresses and thermal fatigue in CrN hard coatings characterized by high-temperature synchrotron X-ray diffraction. Thin Solid Films, 2010, 518, 2090-2096.	0.8	27
166	Effect of Pt nanoparticle decoration on the H2 storage performance of plasma-derived nanoporous graphene. Carbon, 2021, 171, 294-305.	5.4	27
167	Materials Engineering for Flexible Metallic Thin Film Applications. Materials, 2022, 15, 926.	1.3	27
168	Interfaces in nanostructured thin films and their influence on hardness. International Journal of Materials Research, 2005, 96, 468-480.	0.8	26
169	Micro- and bonding structure of arc-evaporated AlCrVN hard coatings. Thin Solid Films, 2008, 516, 6151-6157.	0.8	26
170	Thermal stability of doped CVD κ-Al2O3 coatings. Surface and Coatings Technology, 2010, 204, 3713-3722.	2.2	26
171	X-ray diffraction analysis of three-dimensional residual stress fields reveals origins of thermal fatigue in uncoated and coated steel. Scripta Materialia, 2010, 62, 774-777.	2.6	26
172	Dry-Blasting of α- and κ-Al2O3 CVD Hard Coatings: Friction Behaviour and Thermal Stress Relaxation. Tribology Letters, 2013, 52, 147-154.	1.2	26
173	Needle grass array of nanostructured nickel cobalt sulfide electrode for clean energy generation. Surface and Coatings Technology, 2018, 354, 306-312.	2.2	26
174	Thermal stability of nanolamellar fcc-Ti1-xAlxN grown by chemical vapor deposition. Acta Materialia, 2019, 174, 195-205.	3.8	26
175	Thermal expansion of magnetron sputtered TiCxN1-x coatings studied by high-temperature X-ray diffraction. Thin Solid Films, 2019, 688, 137307.	0.8	26
176	Anisotropy of fracture toughness in nanostructured ceramics controlled by grain boundary design. Materials and Design, 2019, 161, 80-85.	3.3	26
177	Surface chemical changes induced by low-energy ion bombardment in chromium nitride layers. Surface and Interface Analysis, 2002, 34, 740-743.	0.8	25
178	Intrinsic stresses and stress relaxation in TiN/Ag multilayer coatings during thermal cycling. Thin Solid Films, 2008, 516, 1920-1924.	0.8	25
179	Elastic constants of fibre-textured thin films determined by X-ray diffraction. Journal of Applied Crystallography, 2009, 42, 416-428.	1.9	25
180	Effects of thermal annealing on the microstructure of sputtered Al2O3 coatings. Journal of Vacuum Science and Technology A: Vacuum, Surfaces and Films, 2011, 29, .	0.9	25

#	Article	IF	CITATIONS
181	PVD and CVD Hard Coatings. , 2014, , 449-467.		25
182	Enhanced Ti0.84Ta0.16N diffusion barriers, grown by a hybrid sputtering technique with no substrate heating, between Si(001) wafers and Cu overlayers. Scientific Reports, 2018, 8, 5360.	1.6	25
183	Stress relaxation through thermal crack formation in CVD TiCN coatings grown on WC-Co with different Co contents. International Journal of Refractory Metals and Hard Materials, 2020, 86, 105102.	1.7	24
184	Corrosion characteristics of plain carbon steel coated with TiN and ZrN under high-flux ion bombardment. Surface and Coatings Technology, 2002, 160, 82-86.	2.2	23
185	Microstructure and mechanical properties of nanocrystalline Al–Cr–B–N thin films. Surface and Coatings Technology, 2012, 213, 1-7.	2.2	23
186	Industrial-scale sputter deposition of Cr1â^'xAlxN coatings with 0.21â‰ ¤ â‰ 0 .74 from segmented targets. Surface and Coatings Technology, 2013, 232, 303-310.	2.2	23
187	Nanoporous spongy graphene: Potential applications for hydrogen adsorption and selective gas separation. Thin Solid Films, 2015, 596, 242-249.	0.8	23
188	Few-step synthesis, thermal purification and structural characterization of porous boron nitride nanoplatelets. Materials and Design, 2016, 110, 540-548.	3.3	23
189	Structure and properties of decorative rare-earth hexaboride coatings. Surface and Coatings Technology, 1996, 86-87, 715-721.	2.2	22
190	Morphology and Microstructure of Hard and Superhard Zr–Cu–N Nanocomposite Coatings. Japanese Journal of Applied Physics, 2002, 41, 6529-6533.	0.8	22
191	Synthesis–structure relations for reactive magnetron sputtered V2O5 films. Surface and Coatings Technology, 2008, 202, 1551-1555.	2.2	22
192	Influence of different atmospheres on the thermal decomposition of Al-Cr-N coatings. Journal Physics D: Applied Physics, 2008, 41, 155316.	1.3	22
193	display="inline"> <mml:msub><mml:mrow /><mml:mn>2</mml:mn></mml:mrow </mml:msub> (100)/Al <mml:math xmlns:mml="http://www.w3.org/1998/Math/MathML" display="inline"><mml:msub><mml:mrow /><mml:mn>2</mml:mn></mml:mrow </mml:msub>O<mml:math< td=""><td>1.1</td><td>22</td></mml:math<></mml:math 	1.1	22
194	Insights into the atomic and electronic structure triggered by ordered nitrogen vacancies in CrN. Physical Review B, 2013, 87, .	1.1	22
195	The peculiarity of the metal-ceramic interface. Scientific Reports, 2015, 5, 11460.	1.6	22
196	Influence of surface topography on early stages on steel galling of coated WC-Co hard metals. International Journal of Refractory Metals and Hard Materials, 2016, 57, 24-30.	1.7	22
197	Boron Nitride Nanotubes Versus Carbon Nanotubes: A Thermal Stability and Oxidation Behavior Study. Nanomaterials, 2020, 10, 2435.	1.9	22
198	Transmission electron microscopy of nanocomposite CrB–N thin films. Vacuum, 2007, 82, 209-213.	1.6	21

#	Article	IF	CITATIONS
199	Deposition of Ti–Al–N coatings by thermal CVD. International Journal of Refractory Metals and Hard Materials, 2008, 26, 563-568.	1.7	21
200	Wear-resistant Ti–B–N nanocomposite coatings synthesized by reactive cathodic arc evaporation. International Journal of Refractory Metals and Hard Materials, 2010, 28, 23-31.	1.7	21
201	Carbon doped α-Al2O3 coatings grown by chemical vapor deposition. Surface and Coatings Technology, 2012, 206, 4771-4777.	2.2	21
202	Electro-mechanical behavior of Al/Mo bilayers studied with in situ straining methods. Thin Solid Films, 2018, 665, 131-136.	0.8	21
203	Nanostructured Fe-Ni Sulfide: A Multifunctional Material for Energy Generation and Storage. Catalysts, 2019, 9, 597.	1.6	21
204	Optical properties and corrosion behaviour of sputtered Zr-B and Zr-B-N coatings. Surface and Coatings Technology, 1993, 60, 571-576.	2.2	20
205	Tribological Properties of Nanocomposite CrC x /a-C:H Thin Films. Tribology Letters, 2007, 27, 97-104.	1.2	20
206	In Situ Studies of TiC1â^'x N x Hard Coating Tribology. Tribology Letters, 2010, 40, 365-373.	1.2	20
207	Influence of Ar ion etching on the surface topography of cemented carbide cutting inserts. International Journal of Refractory Metals and Hard Materials, 2017, 69, 234-239.	1.7	20
208	Sputtered thermionic hexaboride coatings. Surface and Coatings Technology, 1998, 98, 1315-1323.	2.2	19
209	Optimization of plasma-assisted chemical vapour deposition hard coatings for their application in aluminium die-casting. Surface and Coatings Technology, 2001, 142-144, 1005-1011.	2.2	19
210	Residual stresses in thermally cycled CrN coatings on steel. Thin Solid Films, 2008, 517, 1167-1171.	0.8	19
211	Energy consumption and material fluxes in hard coating deposition processes. Surface and Coatings Technology, 2016, 299, 49-55.	2.2	19
212	Improvement of oxidation and corrosion resistance of Mo thin films by alloying with Ta. Thin Solid Films, 2016, 599, 1-6.	0.8	19
213	Thermal stability of immiscible sputter-deposited Cu-Mo thin films. Journal of Alloys and Compounds, 2019, 783, 208-218.	2.8	19
214	Low-friction PACVD TiN coatings: influence of Cl-content and testing conditions on the tribological properties. Surface and Coatings Technology, 2003, 174-175, 450-454.	2.2	18
215	Accurate Raman spectroscopy of diamond-like carbon films deposited by an anode layer source. Diamond and Related Materials, 2008, 17, 1647-1651.	1.8	18
216	Oxidation and diffusion processes during annealing of AlCrVN hard coatings. Journal of Vacuum Science and Technology A: Vacuum, Surfaces and Films, 2008, 26, 302-308.	0.9	18

#	Article	IF	CITATIONS
217	Thermally-induced formation of hexagonal AlN in AlCrN hard coatings on sapphire: Orientation relationships and residual stresses. Surface and Coatings Technology, 2010, 205, 1320-1323.	2.2	18
218	Influence of varying nitrogen partial pressures on microstructure, mechanical and optical properties of sputtered TiAlON coatings. Acta Materialia, 2016, 119, 26-34.	3.8	18
219	Industrial-scale sputter deposition of molybdenum oxide thin films: Microstructure evolution and properties. Journal of Vacuum Science and Technology A: Vacuum, Surfaces and Films, 2017, 35, .	0.9	18
220	Compressive and tensile bending of sputter deposited Al/Mo bilayers. Scripta Materialia, 2019, 162, 367-371.	2.6	18
221	Sputter deposition of decorative coatings based on ZrB2 and ZrB12. Surface and Coatings Technology, 1992, 54-55, 329-334.	2.2	17
222	Structure and electron emission characteristics of sputtered lanthanum hexaboride films. Surface and Coatings Technology, 1995, 74-75, 890-896.	2.2	17
223	Thermal stability and age hardening of supersaturated AlCrN hard coatings. International Heat Treatment and Surface Engineering, 2007, 1, 75-79.	0.2	17
224	Synthesis and characterization of Cr–B–N coatings deposited by reactive arc evaporation. Journal of Materials Research, 2008, 23, 3048-3055.	1.2	17
225	Can micro-compression testing provide stress–strain data for thin films?. Thin Solid Films, 2009, 518, 1517-1521.	0.8	17
226	A comparative study on Ti1â^'xAlxN coatings reactively sputtered from compound and from mosaic targets. Surface and Coatings Technology, 2011, 205, 4705-4710.	2.2	17
227	Influence of Fe impurities on structure and properties of arc-evaporated AlCrN coatings. Surface and Coatings Technology, 2013, 215, 96-103.	2.2	17
228	A combinatorial X-ray sub-micron diffraction study of microstructure, residual stress and phase stability in TiAlN coatings. Surface and Coatings Technology, 2014, 257, 108-113.	2.2	17
229	Mechanical and tribological properties of AlTiN/AlCrBN multilayer films synthesized by cathodic arc evaporation. Surface and Coatings Technology, 2014, 246, 57-63.	2.2	17
230	Deformation behavior of Re alloyed Mo thin films on flexible substrates: In situ fragmentation analysis supported by first-principles calculations. Scientific Reports, 2017, 7, 7374.	1.6	17
231	Nanoscale residual stress and microstructure gradients across the cutting edge area of a TiN coating on WC Co. Scripta Materialia, 2020, 182, 11-15.	2.6	17
232	Bond strength between TiN coating and microstructural constituents of a high speed steel determined by first principle calculations. Acta Materialia, 2022, 222, 117439.	3.8	17
233	Decorative boride coatings based on LaB6. Surface and Coatings Technology, 1995, 74-75, 1020-1027.	2.2	16
234	Characterization of Nanocomposite Coatings in the System Ti-B-N by Analytical Electron Microscopy and X-Ray Photoelectron Spectroscopy. Monatshefte Für Chemie, 2002, 133, 837-848.	0.9	16

#	Article	IF	CITATIONS
235	Sputter-deposited Al–Au coatings. Intermetallics, 2004, 12, 579-587.	1.8	16
236	Rapid determination of stress factors and absolute residual stresses in thin films. Journal of Applied Crystallography, 2006, 39, 777-783.	1.9	16
237	The relationship between structure and mechanical properties of hydrogenated amorphous carbon films. Diamond and Related Materials, 2010, 19, 1245-1248.	1.8	16
238	Oxidation behavior of arc evaporated Al-Cr-Si-N thin films. Journal of Vacuum Science and Technology A: Vacuum, Surfaces and Films, 2012, 30, .	0.9	16
239	Effect of wavelength modulation of arc evaporated Ti–Al–N/Ti–Al–V–N multilayer coatings on microstructure and mechanical/tribological properties. Thin Solid Films, 2015, 581, 20-24.	0.8	16
240	Theory-guided metal-decoration of nanoporous carbon for hydrogen storage applications. Surface and Coatings Technology, 2018, 351, 42-49.	2.2	16
241	Exceptional fracture resistance of ultrathin metallic glass films due to an intrinsic size effect. Scientific Reports, 2019, 9, 8281.	1.6	16
242	Multi-scale interface design of strong and damage resistant hierarchical nanostructured materials. Materials and Design, 2020, 196, 109169.	3.3	16
243	Adhesion evaluation of thin films to dielectrics in multilayer stacks: A comparison of four-point bending and stressed overlayer technique Materials and Design, 2021, 200, 109451.	3.3	16
244	Identification of cracks generated by indentation experiments in hard-coating systems. Surface and Coatings Technology, 1998, 107, 65-75.	2.2	15
245	The response of PACVD TiN coatings to tribological tests with different counterparts. Wear, 2004, 256, 95-99.	1.5	15
246	Interface structure of epitaxial (111) VN films on (111) MgO substrates. Thin Solid Films, 2008, 517, 1177-1181.	0.8	15
247	Microstructure modifications of CrN coatings by pulsed bias sputtering. Surface and Coatings Technology, 2012, 206, 4666-4671.	2.2	15
248	Restrictions of stress measurements using the curvature method by thermally induced plastic deformation of silicon substrates. Surface and Coatings Technology, 2015, 274, 68-75.	2.2	15
249	Mechanical property enhancement in laminates through control of morphology and crystal orientation. Journal Physics D: Applied Physics, 2015, 48, 295303.	1.3	15
250	Copper diffusion into single-crystalline TiN studied by transmission electron microscopy and atom probe tomography. Thin Solid Films, 2015, 574, 103-109.	0.8	15
251	Resolving depth evolution of microstructure and hardness in sputtered CrN film. Thin Solid Films, 2015, 581, 75-79.	0.8	15
252	Cross-sectional characterization techniques as the basis for knowledge-based design of graded CVD TiN-TiB 2 coatings. International Journal of Refractory Metals and Hard Materials, 2018, 71, 280-284.	1.7	15

#	Article	IF	CITATIONS
253	Antibacterial Silicon Oxide Thin Films Doped with Zinc and Copper Grown by Atmospheric Pressure Plasma Chemical Vapor Deposition. Nanomaterials, 2019, 9, 255.	1.9	15
254	Improved fracture resistance of Cu/Mo bilayers with thickness tailoring. Scripta Materialia, 2021, 202, 113994.	2.6	15
255	Semi-quantitative chemical analysis of hard coatings by Raman micro-spectroscopy: the aluminium chromium nitride system as an example. Analytical and Bioanalytical Chemistry, 2007, 389, 1569-1576.	1.9	14
256	Epitaxial growth of Al–Cr–N thin films on MgO(111). Thin Solid Films, 2008, 517, 598-602.	0.8	14
257	N-K electron energy-loss near-edge structures for TiN/VN layers: an ab initio and experimental study. Analytical and Bioanalytical Chemistry, 2008, 390, 1447-1453.	1.9	14
258	Oxidation and diffusion study on AlCrVN hard coatings using oxygen isotopes 16O and 18O. Thin Solid Films, 2011, 519, 3974-3981.	0.8	14
259	Tailoring age hardening of Ti1â^'xAlxN by Ta alloying. Journal of Vacuum Science and Technology A: Vacuum, Surfaces and Films, 2017, 35, .	0.9	14
260	Novel combustion synthesis of carbon foam‑aluminum fluoride nanocomposite materials. Materials and Design, 2018, 144, 222-228.	3.3	14
261	Role of layer order on the equi-biaxial behavior of Al/Mo bilayers. Scripta Materialia, 2021, 194, 113656.	2.6	14
262	Thermal annealing of sputtered Al–Si–Cu–N films. Vacuum, 2003, 72, 21-28.	1.6	13
263	Current developmental status of thermoelectric (QVD) detectors. Nuclear Instruments and Methods in Physics Research, Section A: Accelerators, Spectrometers, Detectors and Associated Equipment, 2004, 520, 36-40.	0.7	13
264	Increased thermal stability of Ti1â^'xAlxN/TiN multilayer coatings through high temperature sputter deposition on powder-metallurgical high-speed steels. Surface and Coatings Technology, 2014, 257, 48-57.	2.2	13
265	Temperature-Dependent Wear Mechanisms for Magnetron-Sputtered AlTiTaN Hard Coatings. ACS Applied Materials & Interfaces, 2014, 6, 15403-15411.	4.0	13
266	Microstructure-controlled depth gradients of mechanical properties in thin nanocrystalline films: Towards structure-property gradient functionalization. Journal of Applied Physics, 2015, 117, .	1.1	13
267	TiN diffusion barrier failure by the formation of Cu3Si investigated by electron microscopy and atom probe tomography. Journal of Vacuum Science and Technology B:Nanotechnology and Microelectronics, 2016, 34, .	0.6	13
268	Microstructure, mechanical properties and cutting performance of Cr 1-y Ta y N single layer and Ti 1-x Al x N/Cr 1-y Ta y N multilayer coatings. International Journal of Refractory Metals and Hard Materials, 2018, 71, 211-216.	1.7	13
269	The sputter performance of an industrial-scale planar Mo-target over its lifetime: Target erosion and film properties. Surface and Coatings Technology, 2020, 381, 125174.	2.2	13
270	Mono-textured nanocrystalline thin films with pronounced stress-gradients: On the role of grain boundaries in the stress evolution. Journal of Applied Physics, 2014, 115, .	1.1	12

#	Article	IF	CITATIONS
271	Effect of discharge power on target poisoning and coating properties in reactive magnetron sputter deposition of TiN. Journal of Vacuum Science and Technology A: Vacuum, Surfaces and Films, 2016, 34, .	0.9	12
272	Non-reactive dc magnetron sputter deposition of Mo-O thin films from ceramic MoOx targets. Surface and Coatings Technology, 2017, 332, 80-85.	2.2	12
273	Stress-controlled decomposition routes in cubic AlCrN films assessed by in-situ high-temperature high-energy grazing incidence transmission X-ray diffraction. Scientific Reports, 2019, 9, 18027.	1.6	12
274	Surface oxidation of nanocrystalline CVD TiB2 hard coatings revealed by cross-sectional nano-analytics and in-situ micro-cantilever testing. Surface and Coatings Technology, 2020, 399, 126181.	2.2	12
275	Substitution of ThO2 by La2O3 additions in tungsten electrodes for atmospheric plasma spraying. International Journal of Refractory Metals and Hard Materials, 2014, 43, 181-185.	1.7	11
276	Sputter deposition of Mo-based multicomponent thin films from rotatable targets: Experiment and simulation. Applied Surface Science, 2018, 455, 1029-1036.	3.1	11
277	Structure-stress relationships in nanocrystalline multilayered Al0.7Cr0.3N/Al0.9Cr0.1N coatings studied by cross-sectional X-ray nanodiffraction. Materials and Design, 2019, 170, 107702.	3.3	11
278	Near-interface cracking in a TiN coated high speed steel due to combined shear and compression under cyclic impact loading. Surface and Coatings Technology, 2020, 394, 125854.	2.2	11
279	Strength ranking for interfaces between a TiN hard coating and microstructural constituents of high speed steel determined by micromechanical testing. Materials and Design, 2021, 204, 109690.	3.3	11
280	Impact of Si on the high-temperature oxidation of AlCr(Si)N coatings. Journal of Materials Science and Technology, 2022, 100, 91-100.	5.6	11
281	Sputtered decorative hard coatings within the system LaB6î—,ZrB2. Journal of Alloys and Compounds, 1996, 239, 183-192.	2.8	10
282	Toward ultimate performance limits of thermoelectric (QVD) detectors. Nuclear Instruments and Methods in Physics Research, Section A: Accelerators, Spectrometers, Detectors and Associated Equipment, 2004, 520, 56-59.	0.7	10
283	High-temperature residual stresses in thin films characterized by x-ray diffraction substrate curvature method. Review of Scientific Instruments, 2007, 78, 036103.	0.6	10
284	Adhesion Tendency of Polymers to Hard Coatings. International Polymer Processing, 2013, 28, 415-420.	0.3	10
285	Microstructure, mechanical and optical properties of TiAlON coatings sputter-deposited with varying oxygen partial pressures. Journal Physics D: Applied Physics, 2016, 49, 025307.	1.3	10
286	Hierarchical Architectures to Enhance Structural and Functional Properties of Brittle Materials. Advanced Engineering Materials, 2017, 19, 1600683.	1.6	10
287	Microstructure and physical properties of sputter-deposited Cu-Mo thin films. Thin Solid Films, 2018, 653, 301-308.	0.8	10
288	Evolution of stress fields during crack growth and arrest in a brittle-ductile CrN-Cr clamped-cantilever analysed by X-ray nanodiffraction and modelling. Materials and Design, 2021, 198, 109365.	3.3	10

#	Article	IF	CITATIONS
289	Synthesis of bulk reactive Ni–Al composites using high pressure torsion. Journal of Alloys and Compounds, 2021, 857, 157503.	2.8	10
290	Reactive interdiffusion of an Al film and a CoCrFeNi high-entropy alloy. Materials and Design, 2022, 216, 110530.	3.3	10
291	Precipitation-based grain boundary design alters Inter- to Trans-granular Fracture in AlCrN Thin Films. Acta Materialia, 2022, 237, 118156.	3.8	10
292	The influence of various process gases on the magnetron sputtering of ZrB12. Thin Solid Films, 1993, 228, 56-59.	0.8	9
293	Plasma CVD of alumina—Unsolved problems. Vacuum, 2005, 80, 141-145.	1.6	9
294	Single-crystal growth of NaCl-structure Al–Cr–N thin films on MgO(001) by magnetron sputter epitaxy. Scripta Materialia, 2007, 57, 1089-1092.	2.6	9
295	Synthesis and characterisation of sputtered hard coatings of Cr–N/MoS _x . Surface Engineering, 2008, 24, 350-354.	1.1	9
296	Morphology characterization and friction coefficient determination of sputtered V2O5 films. Thin Solid Films, 2010, 519, 1416-1420.	0.8	9
297	Cold pilgering of duplex steel tubes: The response of austenite and ferrite to excessive cold deformation up to high strains. Materials Characterization, 2017, 128, 257-268.	1.9	9
298	Arc evaporated Ti-Al-N/Cr-Al-N multilayer coating systems for cutting applications. International Journal of Refractory Metals and Hard Materials, 2018, 72, 83-88.	1.7	9
299	Linking erosion and sputter performance of a rotatable Mo target to microstructure and properties of the deposited thin films. Surface and Coatings Technology, 2018, 352, 354-359.	2.2	9
300	Evolution of microstructure and mechanical properties of a graded TiAlON thin film investigated by cross-sectional characterization techniques. Surface and Coatings Technology, 2019, 359, 155-161.	2.2	9
301	Reactively sputtered TiN/SiO2 multilayer coatings with designed anisotropic thermal conductivity – From theoretical conceptualization to experimental validation. Surface and Coatings Technology, 2020, 393, 125763.	2.2	9
302	A comparative study on the evaluation of the tribological behaviour of polymer/zinc coated steel sheets. Wear, 1997, 210, 88-95.	1.5	8
303	Utilizing bipolar pulsed PACVD for the deposition of alumina hard coatings. Surface and Coatings Technology, 2004, 188-189, 281-286.	2.2	8
304	TOF-SIMS depth profiling and element mapping on oxidized AlCrVN hard coatings. Analytical and Bioanalytical Chemistry, 2009, 393, 1857-1861.	1.9	8
305	C2H6 as precursor for low pressure chemical vapor deposition of TiCNB hard coatings. Surface and Coatings Technology, 2013, 215, 127-132.	2.2	8
306	V-alloyed ZrO2 coatings with temperature homogenization function for high-temperature sliding contacts. Surface and Coatings Technology, 2013, 228, 76-83.	2.2	8

#	Article	IF	CITATIONS
307	Arc-produced short-length multi-walled carbon nanotubes as "millstones―for the preparation of graphene-like nanoplatelets. Carbon, 2019, 146, 779-784.	5.4	8
308	Balancing the electro-mechanical and interfacial performance of Mo-based alloy films. Materialia, 2020, 12, 100774.	1.3	8
309	Influence of spinodal decomposition and fcc→w phase transformation on global and local mechanical properties of nanolamellar CVD fcc-Ti1-xAlxN coatings. Materialia, 2020, 11, 100696.	1.3	8
310	Microstructural Effects on the Interfacial Adhesion of Nanometer-Thick Cu Films on Glass Substrates: Implications for Microelectronic Devices. ACS Applied Nano Materials, 2021, 4, 61-70.	2.4	8
311	Investigation on structure and properties of arc-evaporated HfAlN hard coatings. Journal of Vacuum Science and Technology A: Vacuum, Surfaces and Films, 2010, 28, 528-535.	0.9	7
312	Tribological Properties of Arc-Evaporated NbAlN Hard Coatings. Tribology Letters, 2012, 45, 143-152.	1.2	7
313	Functional Thin Films for Display and Microelectronics Applications. BHM-Zeitschrift Fuer Rohstoffe Geotechnik Metallurgie Werkstoffe Maschinen-Und Anlagentechnik, 2015, 160, 231-234.	0.4	7
314	Combinatorial synthesis of Cr _{1 â^' x} Al _x N and Ta _{1 â^' x} coatings using industrial scale co-sputtering. Surface Engineering, 2016, 32, 252-257.	Al _{x<}	/sub>N
315	Effect of growth conditions on interface stability and thermophysical properties of sputtered Cu films on Si with and without WTi barrier layers. Journal of Vacuum Science and Technology B:Nanotechnology and Microelectronics, 2017, 35, .	0.6	7
316	A comparative study on NbOx films reactively sputtered from sintered and cold gas sprayed targets. Applied Surface Science, 2018, 436, 1157-1162.	3.1	7
317	Plasma-Derived Graphene-Based Materials for Water Purification and Energy Storage. Journal of Carbon Research, 2019, 5, 16.	1.4	7
318	Crack deflecting microstructure for improved electro-mechanical lifetimes of flexible systems. Materials Letters, 2019, 244, 47-49.	1.3	7
319	Rapid solidification and metastable phase formation during surface modifications of composite Al-Cr cathodes exposed to cathodic arc plasma. Journal of Materials Science and Technology, 2021, 94, 147-163.	5.6	7
320	Design of Nanostructured Hard Coatings for Optimum Performance. Key Engineering Materials, 2004, 264-268, 453-458.	0.4	6
321	Nitrogen atom shift and the structural change in chromium nitride. Acta Materialia, 2015, 98, 119-127.	3.8	6
322	Effects of bias pulse frequencies on reactively sputter deposited NbOx films. Thin Solid Films, 2018, 660, 335-342.	0.8	6
323	Correlation of mechanical damage and electrical behavior of Al/Mo bilayers subjected to bending. Thin Solid Films, 2019, 687, 137480.	0.8	6
324	Sputter deposition of decorative coatings based on ZrB2 and ZrB12. Surface and Coatings Technology, 1992, 54-55, 329-334.	2.2	6

#	Article	IF	CITATIONS
325	Combined ab-initio and N-K, Ti-L ₂ ,3, V-L ₂ ,3 electron energy-loss near edge structure studies for TiN and VN films. International Journal of Materials Research, 2007, 98, 1060-1065.	0.1	5
326	Self-lubricating chromium carbide/amorphous hydrogenated carbon nanocomposite coatings: A new alternative to tungsten carbide/amorphous hydrogenated carbon. Proceedings of the Institution of Mechanical Engineers, Part J: Journal of Engineering Tribology, 2009, 223, 751-757.	1.0	5
327	Atomic and electronic structures of a transition layer at the CrN/Cr interface. Journal of Applied Physics, 2011, 110, 043524.	1.1	5
328	Complementary High Spatial Resolution Methods in Materials Science and Engineering. Advanced Engineering Materials, 2017, 19, 1600671.	1.6	5
329	A correlative experimental and ab initio approach to improve the fracture behavior of Mo thin films by alloying with Cu. Applied Physics Letters, 2017, 111, 134101.	1.5	5
330	Chemical composition and properties of MoAl thin films deposited by sputtering from MoAl compound targets. Journal of Vacuum Science and Technology A: Vacuum, Surfaces and Films, 2017, 35, 041504.	0.9	5
331	Improved electro-mechanical reliability of flexible systems with alloyed Mo-Ta adhesion layers. Thin Solid Films, 2021, 720, 138533.	0.8	5
332	Evolution of structure, residual stress, thermal stability and wear resistance of nanocrystalline multilayered Al0.7Cr0.3N-Al0.67Ti0.33N coatings. Surface and Coatings Technology, 2021, 425, 127712.	2.2	5
333	Some Materials Science Aspects of PVD Hard Coatings. , 2001, , 263-274.		5
334	Thermal Stability of Advanced Nanostructured Wear-Resistant Coatings. Nanostructure Science and Technology, 2006, , 464-510.	0.1	5
335	Low-Friction Mechanisms Active for Carbon Containing Coatings: Ti-C-N as a Model System. BHM-Zeitschrift Fuer Rohstoffe Geotechnik Metallurgie Werkstoffe Maschinen-Und Anlagentechnik, 2008, 153, 263-267.	0.4	4
336	Structure, Stresses and Stress Relaxation of TiN/Ag Nanocomposite Films. Journal of Nanoscience and Nanotechnology, 2009, 9, 3606-3610.	0.9	4
337	Synthesis and characterisation of sputtered hard coatings within the system Cr–N/WS _X . Surface Engineering, 2010, 26, 602-606.	1.1	4
338	Fabry-PÃf©rot-based thin film structure used as IR-emitter of an NDIR gas sensor: ray tracing simulations and measurements. Proceedings of SPIE, 2011, , .	0.8	4
339	Influence of discharge power and bias potential on microstructure and hardness of sputtered amorphous carbon coatings. Journal of Vacuum Science and Technology A: Vacuum, Surfaces and Films, 2018, 36, 021501.	0.9	4
340	Nanoscale stress distributions and microstructural changes at scratch track cross-sections of a deformed brittle-ductile CrN-Cr bilayer. Materials and Design, 2020, 195, 109023.	3.3	4
341	Sputter deposition of NiW films from a rotatable target. Applied Surface Science, 2020, 511, 145616.	3.1	4
342	Characterization of Nanocomposite Coatings in the System Ti-B-N by Analytical Electron Microscopy		4

and X-Ray Photoelectron Spectroscopy. , 2002, , 101-112.

#	Article	IF	CITATIONS
343	LaB6-based, Zr-alloyed, decorative hard coatings. Thin Solid Films, 1996, 286, 188-195.	0.8	3
344	Tribological behaviour of plasma nitrided and plasma sulfonitrided cold work steels. Surface Engineering, 2004, 20, 474-478.	1.1	3
345	Influence of hydrogen sulfide addition on the alumina deposition by plasma CVD. Surface and Coatings Technology, 2005, 200, 360-363.	2.2	3
346	Transmission electron microscopy characterization of CrN films on MgO(001). Thin Solid Films, 2013, 545, 154-160.	0.8	3
347	Oxidation and wet etching behavior of sputtered Mo-Ti-Al films. Journal of Vacuum Science and Technology A: Vacuum, Surfaces and Films, 2018, 36, .	0.9	3
348	Molecular Coverage Determines Sliding Wear Behavior of n-Octadecylphosphonic Acid Functionalized Cu–O Coated Steel Disks against Aluminum. Materials, 2020, 13, 280.	1.3	3
349	Morphology of cracks and shear bands in polymer-supported thin film metallic glasses. Materials Today Communications, 2021, 28, 102547.	0.9	3
350	Duplex processing for increased adhesion of sputter deposited Ti1-xAlxN coatings on a Fe–25%Co–15%Mo tool material. Surface and Coatings Technology, 2012, 206, 3601-3606.	2.2	2
351	Friction reduction by thermal treatment of arc evaporated TiAlTaN coatings in methane. Tribology International, 2013, 67, 54-60.	3.0	2
352	Tribological testing of leather surface coated with sputter-deposited Ti-Ag-O films. Tribology International, 2019, 137, 59-65.	3.0	2
353	Angular resolved mass-energy analysis of species emitted from a dc magnetron sputtered NiW-target. Journal of Vacuum Science and Technology A: Vacuum, Surfaces and Films, 2020, 38, 023401.	0.9	2
354	Film thickness and architecture effects in biaxially strained polymer supported Al/Mo bilayers. Materials Today Communications, 2022, 31, 103455.	0.9	2
355	Influence of matrix composition and MC carbide content on damage behaviour of TiN-coated high speed steel due to cyclic shear and compression load. Surface and Coatings Technology, 2022, 442, 128546.	2.2	2
356	Temperature Dependence of Residual Stress Gradients in Shot-Peened Steel Coated with CrN. Materials Science Forum, 2008, 571-572, 101-106.	0.3	1
357	Structure, stresses and stress relaxation of TiN/Cu multilayer and nanocomposite coatings. International Journal of Materials Research, 2009, 100, 1114-1118.	0.1	1
358	Advanced Engineering Materials 4â^•2017. Advanced Engineering Materials, 2017, 19, 1700108.	1.6	1
359	Oxidation and wet-etching behavior of MoAlTi thin films deposited by sputtering from a rotatable MoAlTi compound target. Journal of Vacuum Science and Technology B:Nanotechnology and Microelectronics, 2019, 37, 021202.	0.6	1
360	Evaluation of anodic coatings on small decorative aluminium parts. Transactions of the Institute of Metal Finishing, 1992, 70, 129-134.	0.6	0

#	Article	IF	CITATIONS
361	Sputtered Coatings Based on the Al2Au Phase. Materials Research Society Symposia Proceedings, 2004, 842, 333.	0.1	0
362	Thermal Stability of Nanostructured TiN-TiB2 Thin Films. Materials Research Society Symposia Proceedings, 2004, 854, U6.2.1.	0.1	0
363	A Comparison of the Electronic Structure of N-K in TiN and VN using EELS and Ab-initio Calculations. Microscopy and Microanalysis, 2007, 13, 414-415.	0.2	Ο
364	A Novel Technique to Determine Elastic Constants of Thin Films. Materials Research Society Symposia Proceedings, 2008, 1139, 1.	0.1	0
365	Tribological Behavior of Sputtered CrAINbN Hard Coatings at Elevated Temperatures. , 2009, , 703-704.		Ο
366	Em. O. UnivProfessor DiplIng. Dr. mont. Dr. h. c. Franz Jeglitsch zum 75. Geburtstag. International Journal of Materials Research, 2009, 100, 1018-1020.	0.1	0
367	Macroscopic Fracture Behaviour of CrN Hard Coatings Evaluated by X-Ray Diffraction Coupled with Four-Point Bending. Materials Science Forum, 2013, 768-769, 272-279.	0.3	Ο
368	Wear behavior of PACVD tin coatings deposited onto tool steels. European Physical Journal Special Topics, 2001, 11, Pr3-893-Pr3-900.	0.2	0
369	50thAnniversary of the Metallurgy Seminar in Arlberg 70thbirthday of Franz Jeglitsch. International Journal of Materials Research, 2004, 95, 570-572.	0.8	Ο
370	Sputter deposition of decorative coatings based on ZrB2 and ZrB12. , 1992, , 329-334.		0